Heliyon 11 (2025) e41961

Contents lists available at ScienceDirect

Heliyon

journal homepage: www.cell.com/heliyon

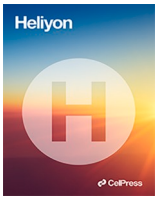

Research article

Cherry tree gum-derived silver/microporous carbon: Reduction of nitroaromatic compounds by microwave-assisted reaction

Hossein Ghafuri *, Fariba Gholipour, Peyman Hanifehnejad, Fatemeh Bijari

Catalysts and Organic Synthesis Research Laboratory, Department of Chemistry, Iran University of Science and Technology, Tehran, 16846-13114, Iran

ARTICLE INFO

Keywords:
Microporous carbon
Ag@MC
Microwave-assisted
Solvent-free
Nitroaromatic reduction

ABSTRACT

In this study, a silver/microporous carbon (Ag@MC) nanocomposite was synthesized using cherry tree gum as a carbon precursor via a hydrothermal method. The catalytic performance of Ag@MC was evaluated for the reduction of nitroaromatic derivatives under solvent-free and microwave-assisted conditions, achieving yields higher than 90 % in just 5 min, significantly shorter than many comparable studies. Comprehensive characterization confirmed the structure and stability of Ag@MC, with silver nanoparticles effectively trapped within its microporous matrix. The nanocomposite demonstrated excellent reusability, maintaining high catalytic activity over six cycles, thereby adhering to green chemistry principles. These findings highlight the potential of using sustainable natural polymers for high-efficiency catalytic applications.

1. Introduction

Water pollution is a critical environmental issue with significant implications for ecosystems, human health, and sustainable development globally. The degradation of water quality affects all forms of life, disrupts ecological balances, and poses direct threats to human health through contaminated drinking water and food sources [1]. Addressing water pollution requires comprehensive strategies that include upgrading and expanding wastewater treatment infrastructure. Such improvements can effectively remove pollutants from sewage and industrial discharges before they are released into the environment [2–4].

Catalysts play a crucial role in enhancing the efficiency and effectiveness of water treatment processes [5,6]. Various catalysts have been employed in the treatment of water pollution, including metal oxides, zeolites, noble metals, enzymes, and biochar. Each of these catalysts offers unique properties that contribute to their effectiveness in different water treatment processe [7–11]. Porous carbon materials are renowned for their exceptional porosity and surface area, making them highly effective in various industrial applications, including gas storage, separation processes, and catalysis [12–14]. These materials offer several advantages over other catalysts, such as enhanced adsorption capacity and catalytic activity due to their extensive network of pores [15,16]. They can be derived from various organic precursors, including natural polymers and biomass, making them versatile and sustainable. Porous carbon materials exhibit excellent chemical and thermal stability, making them suitable for a wide range of environmental conditions. Additionally, the use of abundant and renewable resources like natural polymers reduces production costs, making these materials economically attractive [17,18]. The synthesis of porous carbon involves the carbonization of organic precursors, such as natural polymers or biomass-derived materials, followed by activation to enhance the porosity and surface properties.

* Corresponding author.
E-mail address: ghafuri@iust.ac.ir (H. Ghafuri).

https://doi.org/10.1016/j.heliyon.2025.e41961
Received 10 September 2024; Received in revised form 28 December 2024; Accepted 13 January 2025
Available online 21 January 2025

Traditional literature often relies on non-renewable or less sustainable sources, whereas cherry tree gum offers an environmentally friendly alternative. Cherry tree gum, derived from the exudate of cherry trees, represents a unique and sustainable source of natural polymer for the synthesis of porous carbon materials [19,20]. Traditional literature often relies on non-renewable or less sustainable sources, whereas cherry tree gum offers an environmentally friendly alternative [21]. Additionally, the carbons produced from cherry tree gum exhibit a high surface area and well-developed porosity, which are critical for applications in adsorption and catalysis [22]. By incorporating cherry tree gum as a precursor for porous carbon synthesis, researchers align with the principles of green chemistry by utilizing a renewable resource, reducing carbon footprint, and promoting the circular economy.

To enhance the properties of porous carbon, various composites with metals such as aluminum, magnesium, titanium, and silver can be synthesized [23,24]. Silver nanoparticles, known for their unique optical, catalytic, and antimicrobial properties, have garnered significant attention in nanotechnology and biomedicine [25,26]. The synergistic combination of silver nanoparticles and porous carbon not only expands the applications of these materials but also offers novel opportunities for tailored properties in areas such as sensing, catalysis, and environmental remediation.

Nitroaromatic derivatives are relatively uncommon and are mainly released into the environment through human activities [27]. These compounds are widely used in industries such as dyes, polymers, and pesticides, leading to soil and groundwater contamination and posing health risks like hepatotoxicity, skin sensitization, and mutagenicity. The stability and electron-withdrawing nature of the nitro group make nitroaromatics resistant to oxidative degradation [28,29]. However, they can be reduced to non-toxic aromatic amines, which are valuable in agrochemicals, dyes, herbicides, pharmaceuticals, chelating agents, and photographic chemicals [30,31]. The reduction of nitroaromatics has been achieved using various catalysts, including CuNi bimetallic nanoparticles, Rh-Fe_3O_4, Pd/C, Au nanocatalysts, Pd/SiO_2, and gum-acacia/Pt [32–36]. Despite their efficacy, there is still a need for more efficient and sustainable methods to reduce nitroaromatic compounds.

Performing reactions under solvent-free conditions can reduce the problems associated with chemical reactions, such as high reaction times, high energy consumption, and waste production. Conventional heating methods often result in poor temperature control and uneven heat distribution within the reaction vessel. Microwave irradiation offers an efficient alternative, directly affecting individual molecules and eliminating the need for solvents. The reduction of nitroaromatic compounds to their corresponding amines is a critical reaction in both industrial and environmental contexts due to the widespread use of these compounds in pharmaceuticals, agrochemicals, and dyes. Despite advancements in catalytic methodologies, several challenges remain prevalent in current catalytic systems. One significant issue is selectivity; many traditional catalytic methods lack the necessary selectivity to differentiate between nitroaromatic compounds and other reducible functionalities within the same molecule, leading to undesirable side reactions and low yields of the target amine products [37]. Another challenge is the toxicity and environmental impact of commonly used catalysts, such as palladium, platinum, and rhodium. These catalysts are effective but not environmentally benign, and their synthesis, usage, and disposal pose significant environmental and health risks [38]. Additionally, the solvents often used in these reactions can be hazardous and contribute to the overall environmental footprint of the process [39]. Lastly, traditional catalytic methods often require harsh reaction conditions, including high temperatures and pressures, which not only increase energy consumption but also limit the types of substrates that can be processed, as some may degrade or react undesirably under these conditions [36].

Our study focused on the reduction of hazardous nitroaromatic compounds using an innovative method that employs Ag@MC under microwave-assisted conditions. This method provided several benefits, including short reaction times, high yields, and solvent-free conditions. By aligning with green chemistry principles, we successfully converted nitroaromatics to their corresponding aromatic amine derivatives. The aim is to demonstrate that this innovative approach not only enhances the efficiency and yield of the reduction process but also aligns with green chemistry principles by utilizing renewable resources and minimizing environmental impact.

2. Materials and methods

2.1. Experimental materials

All chemicals were purchased by Sigma–Aldrich and Merck companies. Many analyses have been performed, including Fourier Transform Infrared Spectroscopy (FT-IR) by Tensor27, Thermal Gravimetric Analysis (TGA) under argon atmosphere was taken by STA 504, Nuclear Magnetic Resonance (NMR) with Varian-Inova 500 MHz, X-Ray Powder Diffraction (XRD) by Dron-8, Energy-Dispersive X-ray (EDS) by Numerix DXP–X10P, Nitrogen adsorption analysis (BET) with ASAP™ micromeritics 2020, and Field Emission Scanning Electron Microscopy (FE-SEM) by TESCAN-MIRA.

2.2. Preparation of cherry tree gum extract

Cherry tree gum (Mw: >5000, from Damavand region of Iran [20]) was collected from the cherry tree, dried in sunlight for two days, and a uniform powder was obtained using a ball mill (2 balls, 30 Hz, 20 min, Retsch Ball-mill). The color of the gum changed from dark yellow to white during this process. Furthermore, the white powder was washed with ethanol several times to remove the impurities and dried completely at 60 °C.

2.3. Preparation of MC

Initially, 2 g of gum powder was carefully added in small increments to a 50 mL round bottom flask containing water. The mixture was stirred continuously until a homogeneous, pure, and clear gel was formed. This gel was then transferred to a 100 mL autoclave

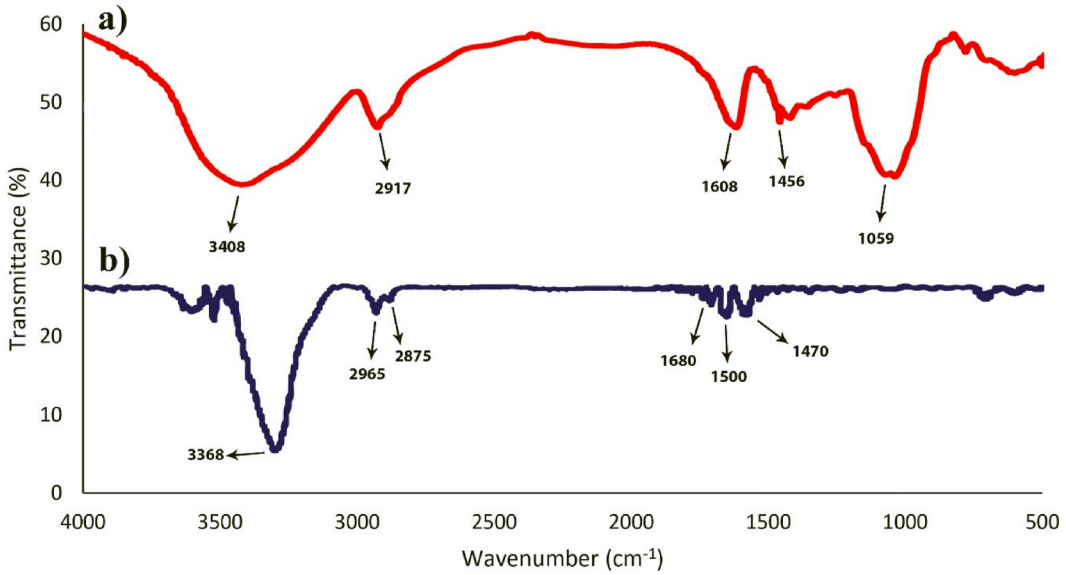

Fig. 1. FT-IR spectrum of (a) cherry tree gum and (b) Ag@MC

flask and subjected to a high temperature of 180 °C in an oven for a duration of 12 h. Following this thermal treatment, the gel transformed into a dark-colored solution. The solution was subsequently filtered to remove any solid impurities and then washed multiple times with water and ethanol to eliminate any residual contaminants. The resulting material was then dried in a vacuum oven at 60 °C for 8 h to remove any remaining moisture and solvents. Then, the obtained powder was carefully mixed with potassium hydroxide in a specific ratio of 1:3. Potassium hydroxide acts as an activating agent crucial for reducing particle size and increasing the surface area of the catalyst. The powder-KOH mixture was then transferred to an oven and exposed to a high temperature of 800 °C for 1 h under a nitrogen atmosphere. Subsequently, the activated powder was thoroughly washed with hydrochloric acid solution (1M) followed by rinsing with water. The washed microporous carbon was then carefully dried in an electric oven at a lower temperature of 110 °C.

2.4. Preparation of Ag@MC

Initially, 0.1 g of silver nitrate ($AgNO_3$) was dissolved in water to prepare a 5 mL solution in a round bottom flask. Subsequently, 0.1 g of MC, was added to the silver nitrate solution. The mixture was then stirred for 2 h under a nitrogen (N_2) atmosphere. Following the stirring period, $NaBH_4$, a potent reducing agent, was gradually added to the mixture in a specific molar ratio of 6:1 ($NaBH_4$: silver nitrate). The addition of $NaBH_4$ initiates the reduction process, converting Ag(II) ions from the silver nitrate into elemental silver nanoparticles (Ag(0)). The mixture containing $NaBH_4$ was further stirred for 6 h to allow complete reduction of the silver ions into metallic silver nanoparticles. The reaction mixture containing the synthesized Ag@MC nanocomposite was carefully filtered to separate the solid material from the liquid phase. The filtered material was then washed sequentially with methanol to remove any residual impurities and unreacted components, followed by rinsing with water to ensure cleanliness. The washed Ag@MC nanocomposite was then subjected to drying at a controlled temperature of 60 °C.

2.5. Reduction of nitroaromatic derivatives

4-chloronitrobenzene (1 mmol) and hydrazine hydrate (10 mmol, 0.972 mL) were accurately measured and combined in a flask. Additionally, 0.03 g of the synthesized catalyst was added to the mixture. The flask containing the reactants and catalyst was then placed in a microwave operating at 100 W. The progress of the chemical reaction was continuously monitored using Thin Layer Chromatography (TLC). Upon reaching the desired reaction endpoint (5–8 min), the catalyst was separated from the reaction mixture by filtration using ethanol. The intended product was then isolated from the reaction mixture either through a simple filtration process or by promoting crystallization.

2.6. Selected spectra data

4-aminoacetophenone (12a): FT-IR (KBr): 3398, 3333, 3223, 1652, 1589, 1440, 1282, 1178 cm^{-1}. NMR (DMSO-d_6): 2.37 (s, 3H, CH_3), 6.03 (s, 2H, NH_2), 6.57 (d, 2H, Ar-H), 7.68 (d, 2H, Ar-H) ppm. (See full images in Supplementary material file)

2-aminobenzophenone (13a): FT-IR (KBr): 3435, 3318, 3166, 1631, 1553, 1448, 1249, 1147, 1024 cm^{-1}. NMR (DMSO-d_6): 6.5 (t,1H, Ar-H), 6.88 (d,1H, Ar-H), 7.13 (s,2H, NH_2), 7.25–7.30 (m, 2H, Ar-H), 7.48–7.59 (m, 5H, Ar-H) ppm. (See full images in

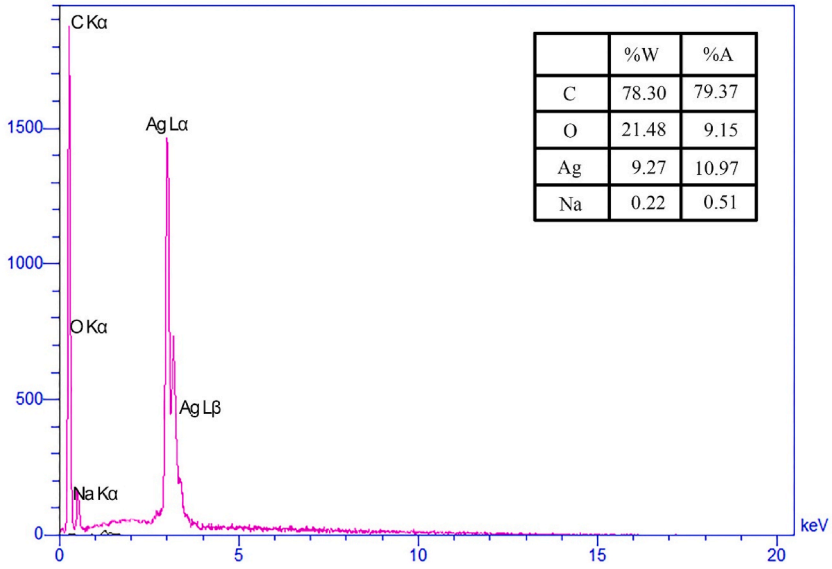

	%W	%A
C	78.30	79.37
O	21.48	9.15
Ag	9.27	10.97
Na	0.22	0.51

Fig. 2. EDS analysis of Ag@MC

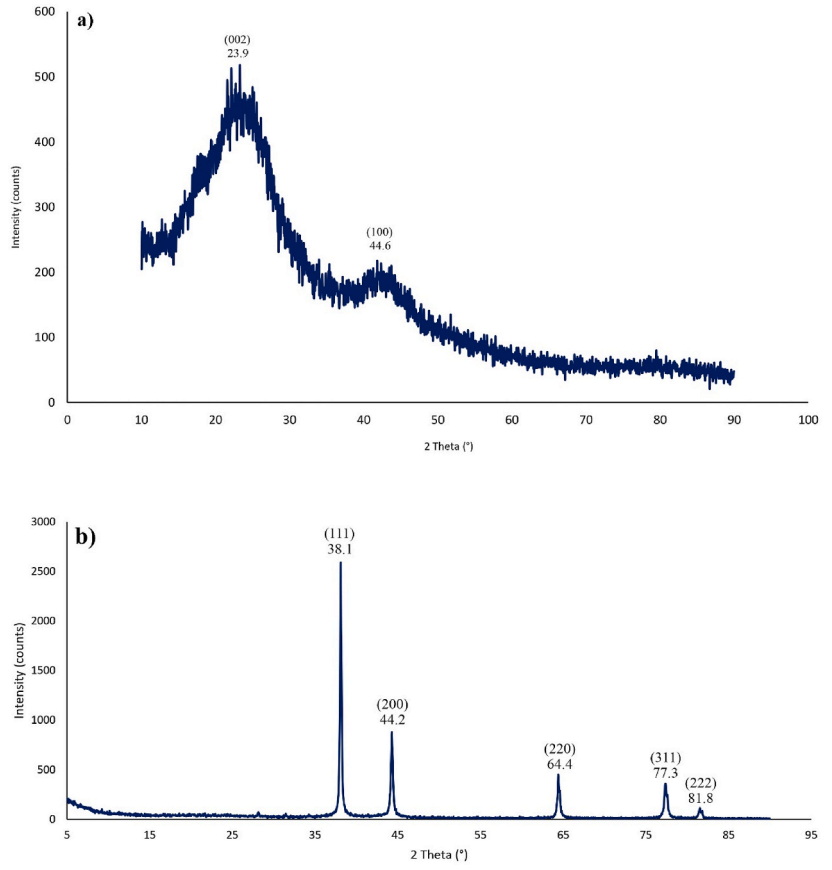

Fig. 3. XRD patterns of a) MC and b) Ag@MC

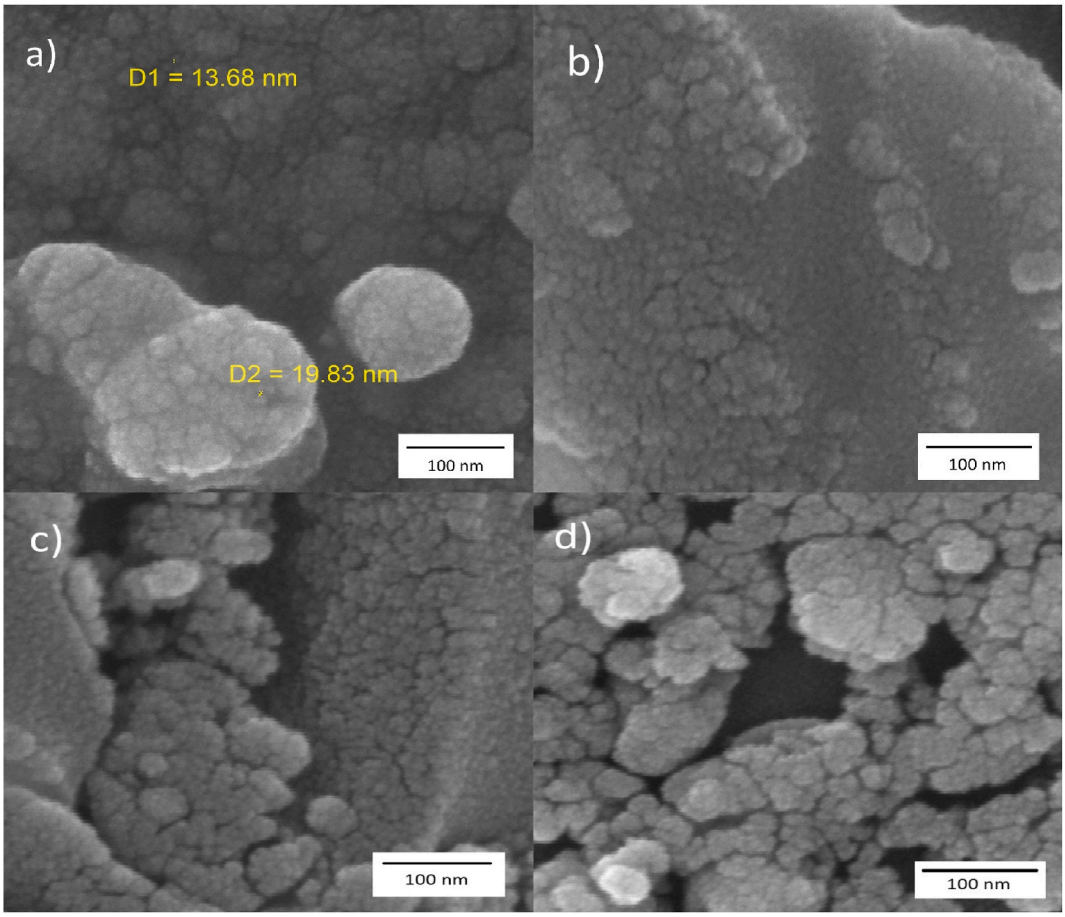

Fig. 4. FE-SEM images (a–c) MC, (d–f) Ag@MC

Supplementary material file)

3. Results and discussion

3.1. Characterization of MC and Ag@MC

The functional groups present in cherry tree gum (Fig. 1-a) and Ag@MC (Fig. 1-b) were identified through FT-IR analysis. In Fig. 1-a, a broad peak about 3408 cm^{-1} was observed, which corresponds to the stretching vibrations of hydroxyl (-OH) groups. Additionally, the stretching vibrations of aliphatic carbon-hydrogen (C-H) groups were observed around 2917 cm^{-1}. The peak at approximately 1608 cm^{-1} corresponds to the stretching vibration of the carbonyl group (C=O), while the peaks at 1456 and 1059 cm^{-1} are attributed to the stretching vibrations of C–O groups. In Fig. 1-b, the infrared spectrum shows a broad peak centered around 3368 cm^{-1} which is indicative of the presence of -OH groups, possibly from adsorbed H_2O molecules. The spectrum also demonstrates the stretching vibrations of aliphatic C-H groups at around 2875 and 2965 cm^{-1}. Moreover, the peaks observed at 1680, 1500, and 1470, as well as at 748 cm^{-1} correspond to stretching vibrations of C=C, Ar C-C, methylene groups, and out-of-plane C-H bending vibrations, respectively [13,40]. These results provide valuable insights into the chemical composition of cherry tree gum and Ag@MC, which may have important implications for their potential applications in various fields.

Although FT-IR analysis is a powerful technique for identifying functional groups, it may not be sensitive enough to detect Ag in a nanocomposite. Therefore, in this research, EDS analysis was employed to confirm the presence of Ag in the prepared nanocomposite (Fig. 2). The high percentage of carbon illustrates that microporous carbon is well prepared, and the washing step leads to removing the potassium. Also, there is an upright percentage of Ag, which means Ag ions are well composited with MC. A small ratio of Na is observed due to the reduction of $AgNO_3$, and it was not washed completely very well after many times.

X-ray diffraction (XRD) analysis was conducted to examine the crystallographic structure of MC (Fig. 3-a) and Ag@MC nanocomposite (Fig. 3-b). In Fig. 3-a, a broad peak centered around 24° is observed, which indicates the amorphous structure of MC, in agreement with the findings reported in the literature [41]. On the other hand, Fig. 3-b displays the wide-angle XRD pattern of Ag@MC, which exhibits a well-crystallized structure. The diffraction peaks observed at 37.9°, 44.1°, 64.3°, and 77.1° correspond to the

Table 1
Specific surface area calculated by analysis, total pore volume, and pore diameter size of MC and Ag@MC

Sample	S^{a}_{BET}/m^2g^{-1}	V^{b}_{p}/cm^3g^{-1}	D^{b}_{p}/nm
MC	1551.73	0.974	1.445
Ag@MC	681.95	0.975	1.923

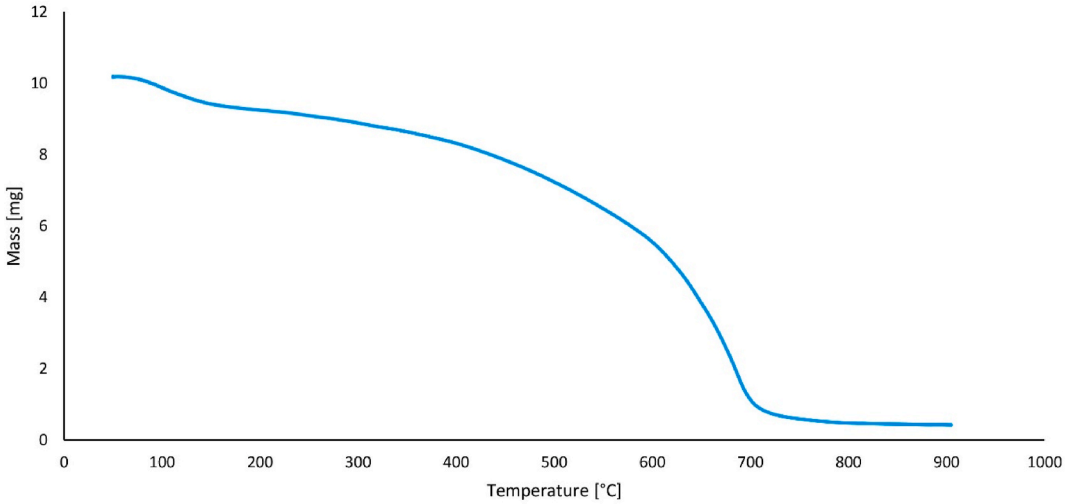

Fig. 5. TGA analysis of Ag@MC

(111), (200), (220), and (311) diffraction reflection planes, respectively [42]. The broad peak typically associated with amorphous carbon may not appear in the XRD pattern of the catalyst due to the dominance of highly crystalline phases in the catalyst, such as metals. These crystalline phases produce strong and sharp diffraction peaks that can overshadow the weaker and broader signals of amorphous carbon, making it less detectable in the XRD pattern [43].

In Fig. 4, we can observe the MC (Fig. 4-a,b) and Ag@MC nanocomposite (Fig. 4-c,d) morphologies, which were analyzed using FE-SEM. The surface of the MC, as shown in Fig. 4(a and b), appears to be agglomerated and rough, with small visible holes that allow Silver with a diameter of 0.133 nm to enter [44]. However, after introducing silver ions into the micro-cavities, the MC structure remained unchanged, and the surface roughness increased, as seen in Fig. 4(c and d). These observations suggest that the introduction of silver ions did not alter the overall structure of MC, but it did affect the surface morphology, which may have implications for the performance of the nanocomposite in various applications.

The surface area, pore size, pore volume, and the type of isotherm were measured by N_2 adsorption-desorption analysis. According to Fig. S1, the N_2 adsorption-desorption isotherm of MC and Ag@MC nanocomposite is type (I), which proves the synthesized nanocomposite has micro pores [45]. The isotherm is relatively flat, and no hysteresis loop is witnessed, suggesting no mesopores are present in the material [46]. The pore size distribution is shown in Table 1, and it is obvious that most of the pores have a diameter of less than 2 nm. Ag@MC has a lower surface area (681.95 m2 g^{-1}) than MC (1551.73 m2 g^{-1}) due to the existence of Ag in the pores of MC. However, the pore diameter of Ag@MC (1.923 nm) is larger than MC (1.445 nm) due to the existence of Ag on the pore apertures of MC.

TGA analysis was performed to evaluate the thermal stability of Ag@MC nanocomposite in the range of 30 °C–800 °C as shown in Fig. 5. Before 100 °C, the mass loss stage may be due to the H_2O adsorbing by synthesized nanocomposite. Ag@MC nanocomposite exhibited excellent thermal resistance and did not experience significant mass reduction up to 350 °C. However, around 600 °C, a significant weight loss was observed, which can be attributed to the decomposition of the synthesized nanocomposite.

3.2. Experimental conditions for the preparation of Ag@MC

The choice of experimental conditions, particularly the temperature and duration for the hydrothermal method, was based on several critical factors aimed at optimizing the synthesis of microporous carbon and ensuring the effectiveness of the resulting catalyst. The hydrothermal treatment at 180 °C for 12 h was selected to ensure the complete conversion of the cherry tree gum into a carbonaceous gel with well-developed porosity. This temperature and duration balance the need for sufficient thermal energy to facilitate the carbonization process while preventing the degradation of the material that could occur at higher temperatures or longer durations. Previous studies have demonstrated that hydrothermal processes at this temperature range are effective in converting natural polymers into porous carbon materials with high surface areas and desirable structural properties [47].

The activation step involving potassium hydroxide (KOH) at 800 °C for 1 h under a nitrogen atmosphere was chosen to maximize

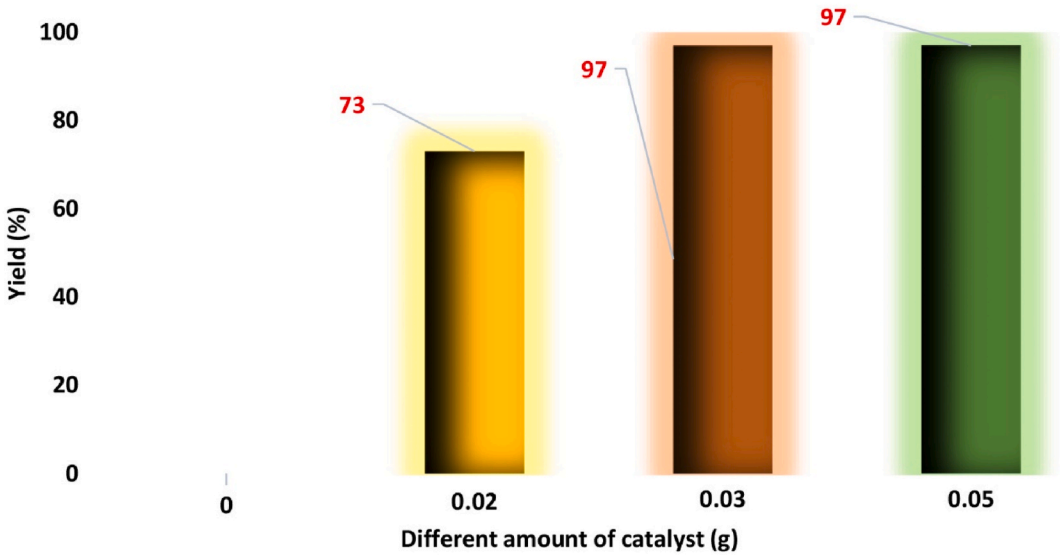

Fig. 6. Effect of the amount of catalyst on the yield of model reaction. Model reaction: 4-chloronitrobenzene (1 mmol), hydrazine hydrate (10 mmol), microwave conditions (100 W), 5 min.
The yields related to the isolated product.

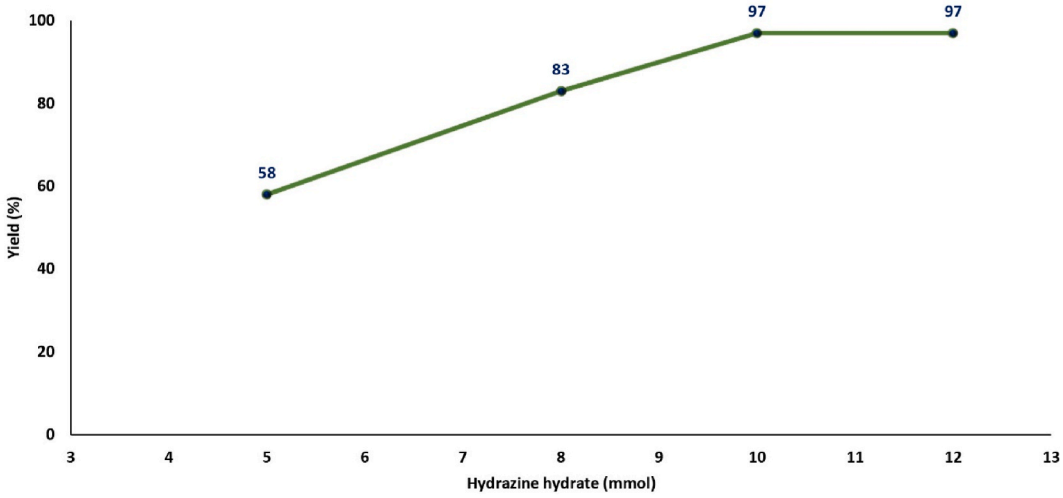

Fig. 7. Effect of the amount of hydrazine hydrate on the yield of model reaction. Model reaction: 4-chloronitrobenzene (1 mmol), catalyst (0.03 g) microwave conditions (100 W), 5 min.
The yields related to the isolated product.

the surface area and porosity of the microporous carbon. The high temperature promotes the activation process, which enhances the material's adsorption capacity and catalytic activity by developing a well-connected network of micropores. KOH is a widely used activating agent that effectively creates a porous structure through chemical activation, and the specified ratio of 1:3 (carbon to KOH) has been shown to produce optimal results in terms of pore development and surface area enhancement [48].

By using a 6:1 M ratio of $NaBH_4$ to $AgNO_3$, this study ensures the efficient production of stable, well-dispersed silver nanoparticles within the microporous carbon matrix, thereby enhancing the catalytic properties of the Ag@MC nanocomposite for the reduction of nitroaromatic compounds [42].

The subsequent washing and drying steps at 60 °C and 110 °C, respectively, ensure the removal of residual activating agents and moisture, preserving the structural integrity of the microporous carbon. These temperatures are sufficient to achieve thorough drying without causing thermal damage to the material, which is crucial for maintaining the high surface area and porosity required for effective catalytic performance [21].

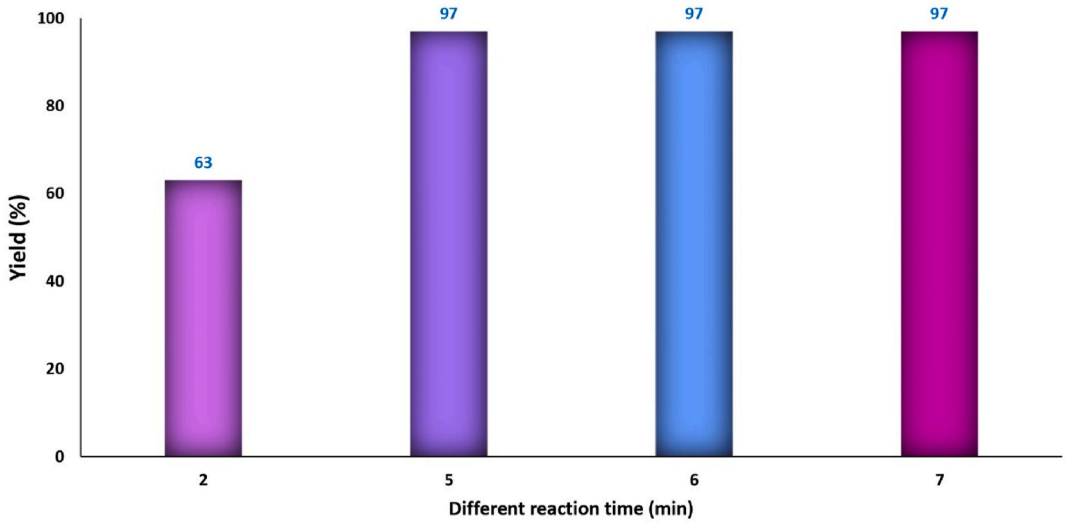

Fig. 8. Effect of reaction time on the yield of model reaction. Model reaction: 4-chloronitrobenzene (1 mmol), hydrazine hydrate (10 mmol), microwave conditions (100 W).
The yields related to the isolated product.

Table 2
Comparison of different reaction conditions[a,b].

Entry	conditions	$N_2H_4.H_2O$ (mmol)	Catalyst (g)	Time (min)	Yield (%)
1	Microwave	10	0.05	5	97
2	Reflux	10	0.03	180	50
3	Sonication	10	0.03	30	40

[a] Reaction conditions: 4-chloronitrobenzene (1 mmol), hydrazine hydrate (10 mmol).
[b] The yields related to the isolated product.

3.3. Microwave-assisted reduction of nitroaromatic derivatives

Our study demonstrates the effective use of cherry tree gum-derived silver/microporous carbon (Ag@MC) nanocomposites for the reduction of nitroaromatic compounds under microwave-assisted, solvent-free conditions. The reduction of these compounds has been carried out with exceptional efficiency using a microwave-assisted approach (100 W) in the presence of 4-chloronitrobenzene (1 mmol), hydrazine hydrate (10 mmol), and the synthesized nanocomposite as a catalyst (0.03 g), which was used as a model reaction. Various parameters were studied to identify the optimal reaction conditions, including reaction time, catalyst and hydrazine hydrate amounts, and diverse reaction conditions. The progress of the reaction was monitored by TLC, and the intended product was easily obtained by simple filtration.

A series of experiments were conducted to determine the optimal amount of catalyst required for the reaction (Fig. 6). Initially, the reaction was carried out without any catalyst, and no product was observed, highlighting the significance of the catalyst in the reaction. Subsequently, the reaction was performed with varying amounts of catalyst, including 0.02, 0.03, and 0.05 g. It was observed that the reaction efficiency increased with the addition of catalysts up to 0.03 g, and there was no further increase in efficiency beyond this point. Therefore, it can be concluded that the optimal amount of catalyst for this particular reaction is 0.03 g.

Several amounts of hydrazine hydrate were tested during the experiment to identify the ideal quantity for the reaction (5, 8, 10, and 12 mmol). The obtained results, displayed in Fig. 7, clearly indicate that the reaction efficiency increases as the amount of hydrazine hydrate increases until it reaches a maximum of 10 mmol. The data suggests that beyond this amount, further increases in the amount of the catalyst do not have any significant impact on the reaction efficiency. As a result, it can be concluded that 10 mmol is the optimal amount of hydrazine hydrate for this specific chemical reaction.

Finally, to determine the most effective reaction time, a study was conducted where different reaction times were tested, including 2, 5, 6, and 7 min (Fig. 8). The experiment aimed to identify the optimal reaction time that would enhance the efficiency of the reaction. After analyzing the results, it was found that the most effective reaction time was 5 min. Interestingly, the study also found that longer reaction times did not improve the reaction efficiency. Hence, it was concluded that 5 min is the optimal reaction time for the studied reaction.

Following the optimization of the reaction, which involved the precise determination of the appropriate amount of catalyst (0.03 g) and hydrazine hydrate (10 mmol), as well as the optimal reaction time (5 min), we went ahead to test different reaction conditions, which included reflux (180 min, 60 % yield) and sonication (30 min, 40 % yield). From the obtained results, as presented in Table 2, it

Table 3
Reduction of nitroaromatic derivatives with optimized reaction conditions.[a].

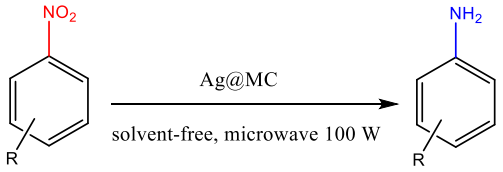

1a-13a

Entry	R	product	Time (min)	Melting point [Ref.]	Yield[b]
1	H	1a	5	–	Oil
2	2-OH	2a	5	171-173 [49]	97
3	4-CH_3	3a	5	51-53 [50]	96
4	4-CH_3OH	4a	5	63-65 [51]	97
5	2-NH_2	5a	5	101-103 [51]	96
6	3-NO_2	6a	7	65-67 [52]	95
7	3-CH_3OH	7a	5	90-93 [49]	96
8	4-NH_2	8a	5	142-144 [51]	96
9	4-OH	9a	5	191-193 [53]	95
10	4-Cl	10a	7	70-71 [54]	94
11	4-COOH	11a	8	187-189 [55]	91
12	4-$COCH_3$	12a	6	104-106 [51]	93
13	2-COPh	13a	5	111-113 [56]	90

[a] Reaction conditions: nitrobenzene (1 mmol), hydrazine hydrate (10 mmol), catalyst (0.03 g), microwave (100 W).
[b] The yields related to the isolated product.

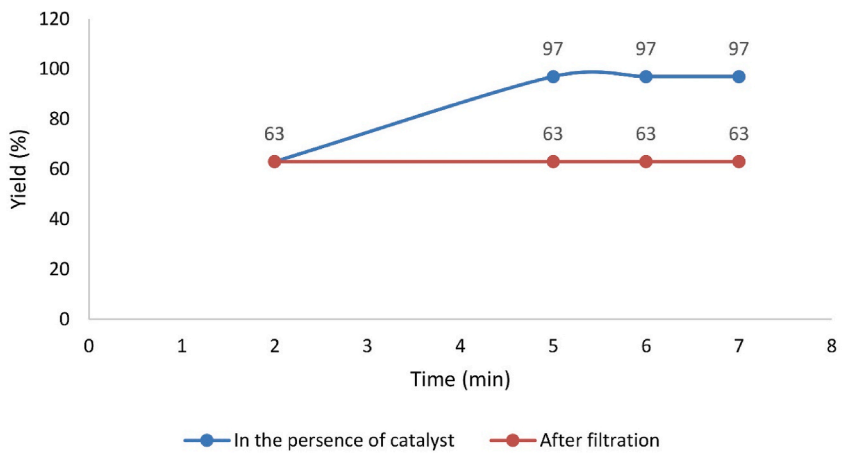

Fig. 9. Hot filtration test to assess catalyst heterogeneity.

is evident that the best reaction conditions were achieved using microwave conditions. This indicates that microwave conditions significantly impact the reaction yield, and it is a better alternative to reflux and sonication.

3.4. Catalytic reduction of various 4-nitroaromatics

In order to showcase the advantageous catalytic properties of Ag@MC, several nitroaromatic derivatives were subjected to experimentation using the optimized conditions. The experiment results revealed that the intended products were produced with a yield ranging from 91 % to 97 % (as indicated in Table 3). This indicates that Ag@MC is a highly effective catalyst for these reactions and can be utilized to produce intended products with a high degree of efficiency.

The leaching study was conducted to evaluate the heterogeneity of the solid catalyst. After 2 min of reaction, the active catalytic species were separated by hot filtration. Monitoring the reaction progress revealed that Ag leaching was negligible (Fig. 9).

3.5. Comparision with other published literature

In comparing the performance of the provided study on cherry tree gum-derived silver/microporous carbon (Ag@MC) for the reduction of nitroaromatic compounds with similar research, it is evident that the provided study exhibits superior performance. The

Table 4
Comparision the reduction reaction conditions of 4-nitrophenol with other published literature.

Entry	Catalyst	Reaction conditions	Time (min)	Yield[a] (%)	Reductant	Ref.
1	Fe_3O_4/CS-Ag	Water, RT	15	98	$NaBH_4$ (0.5 mM)	[57]
2	Fe_3O_4@CS@MS@A	Water, RT	10	98	$NaBH_4$ (1 mM)	[58]
3	QCRAg nanocomposite	Water, RT	30	95	$NaBH_4$ (0.03 M)	[59]
4	Ag@MC	Solvent-free, microwave (100 W)	5	95	hydrazine hydrate (10 mmol)	This work

[a] Isolated yield.

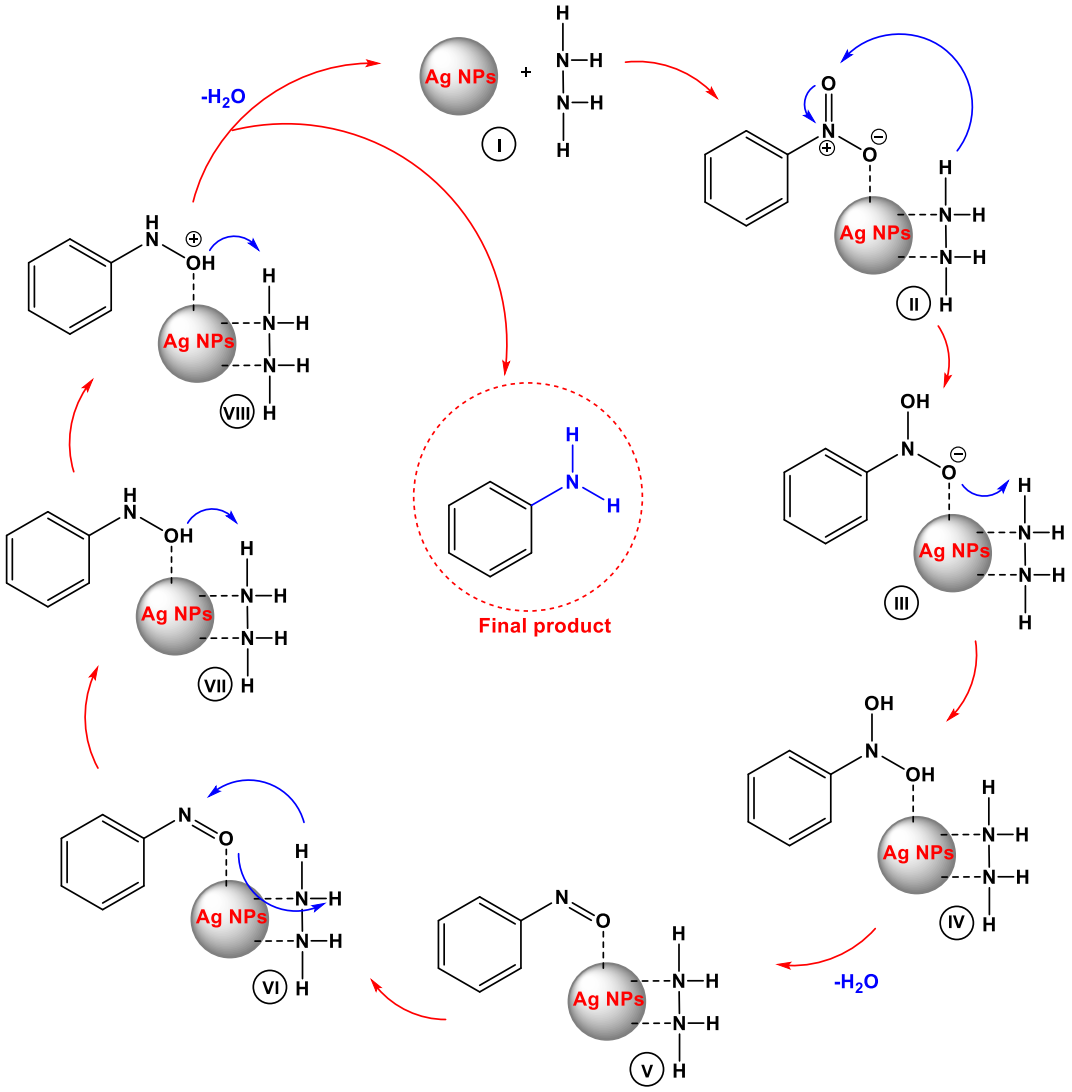

Fig. 10. Mechanism of reduction of nitroaromatic derivatives.

study achieves a significantly shorter reaction time, successfully reducing nitroaromatic compounds in just 5 min under microwave-assisted, solvent-free conditions, while many comparable studies report longer reaction times. For instance, the study by Xu et al. requires 15 min for the reduction process.

Furthermore, the provided study reports yields exceeding 90 %, which is notably higher than those achieved in other studies. For example, Hasan et al. reported a yield of 90 % under similar conditions. The reusability of the Ag@MC nanocomposite is another critical advantage. It maintained high catalytic activity over six cycles, whereas many other nanocomposites showed reduced efficiency after fewer cycles. Ling et al. demonstrated that their nanocomposite maintained activity after ten cycles, but this still reflects the robust performance of the Ag@MC nanocomposite.

Additionally, the use of sustainable natural polymers, such as cherry tree gum, aligns with green chemistry principles, offering an

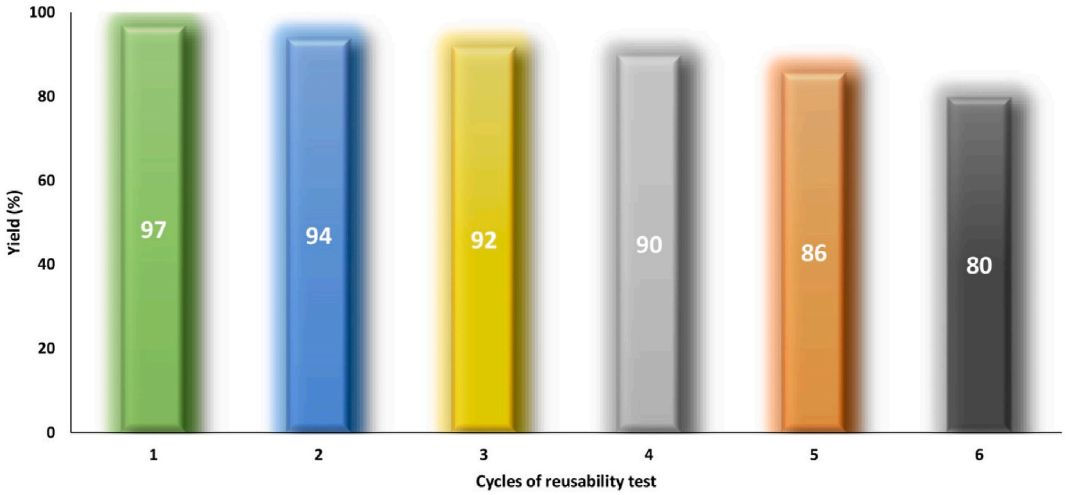

Fig. 11. Reusability of Ag@MC nanocomposite.

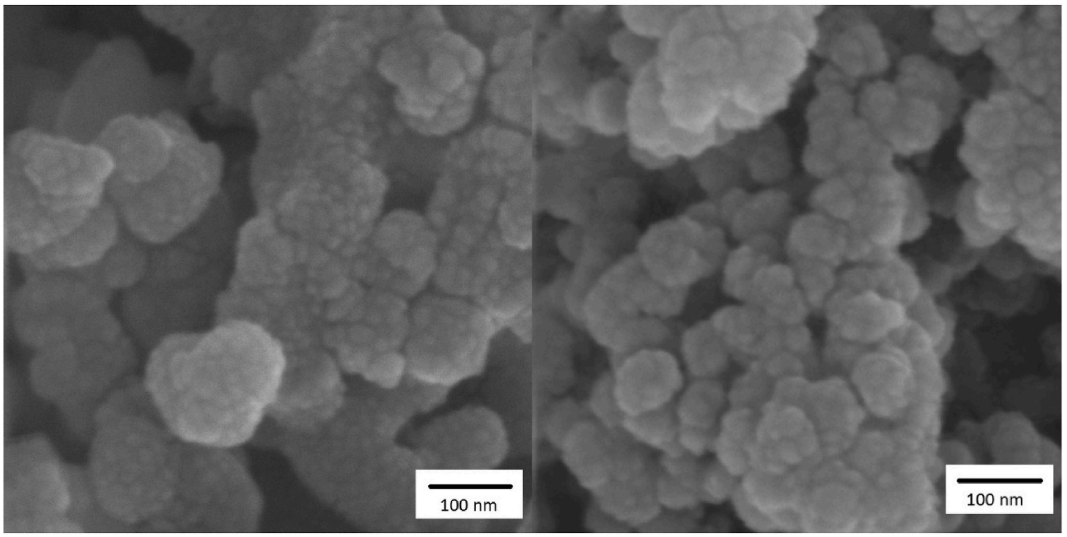

Fig. 12. FE-SEM images of reused Ag@MC

environmentally friendly alternative to the non-renewable resources used in many other studies. This sustainable approach not only reduces the carbon footprint but also promotes the circular economy, providing a distinct advantage over traditional methods.

Overall, the provided study demonstrates superior efficiency, higher yields, greater reusability, and sustainable resource utilization, making it a significant advancement in the field of catalytic reduction of nitroaromatic compounds (See Table 4). This highlights the potential of natural polymer-based nanocomposites in sustainable catalytic applications, setting a benchmark for future research in this area.

3.6. Mechanism

Based on the results of this study and previous literature, the proposed mechanism (Fig. 10) explains the reaction process step-by-step [60,61]. The first step involves the attachment of hydrazine hydrate to Ag NPs. In steps II and III, the oxygens of nitrobenzene bond with hydrogens to form hydroxyl groups. In step IV, a water molecule is eliminated, and a double bond is formed, leading to the production of nitrosobenzene in step V. Moving on to step VI, the nitrogen and oxygen bond with hydrogens of hydrazine hydrate to form hydrogen bonds. Steps VII and VIII involve the hydroxyl group reacting with hydrogen atoms, releasing water. Once water is eliminated, Aniline is produced, and the composite can be reused in the next step. Overall, the proposed mechanism provides a detailed explanation of the reaction process and sheds light on the underlying chemistry behind it.

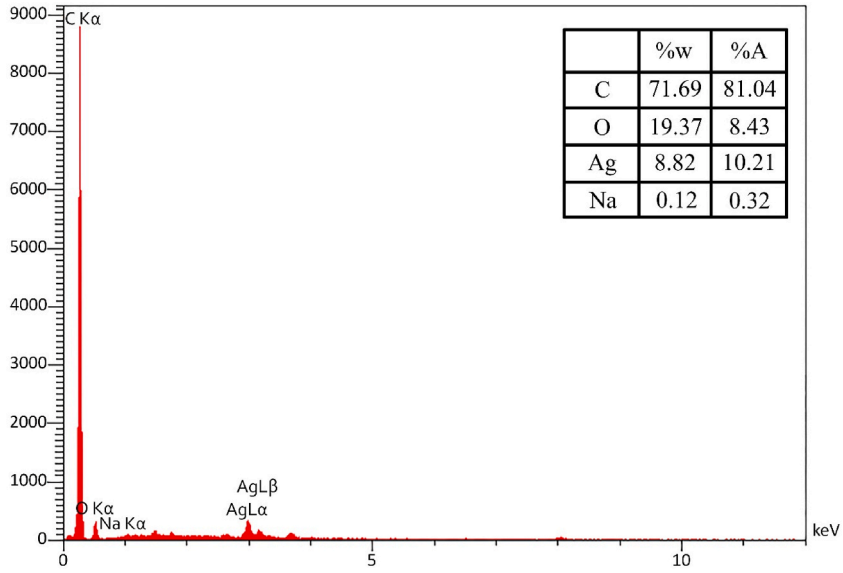

	%w	%A
C	71.69	81.04
O	19.37	8.43
Ag	8.82	10.21
Na	0.12	0.32

Fig. 13. EDS analysis of reused Ag@MC

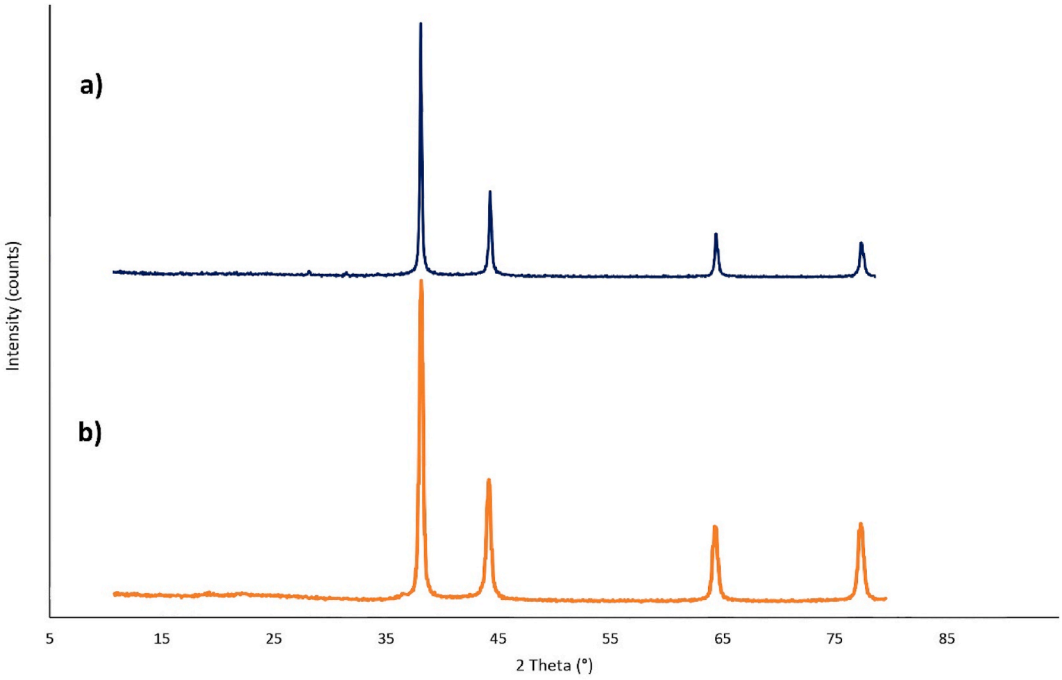

Fig. 14. XRD patterns of a) Ag@MC and b) reused Ag@MC

3.7. Reusability

One of the fundamental principles of green chemistry is the ability to recover and recycle materials. In line with this principle, the reusability of the nanocomposite Ag@MC was studied to reduce nitroaromatics to aromatic amine derivatives. The process involved extracting Ag@MC from the reaction through a simple filtration, washing with water and ethanol, and drying at 70 °C. This process was repeated six times under unchanged conditions. Although the yield gradually decreased after each reaction, the decrease was still within an acceptable range. This study highlights the potential of Ag@MC to be used as an efficient and sustainable catalyst in various chemical reactions (Fig. 11). The FE-SEM, EDS, XRD, and FT-IR analysis of reused catalyst were shown in Figs. 12–15, respectively.

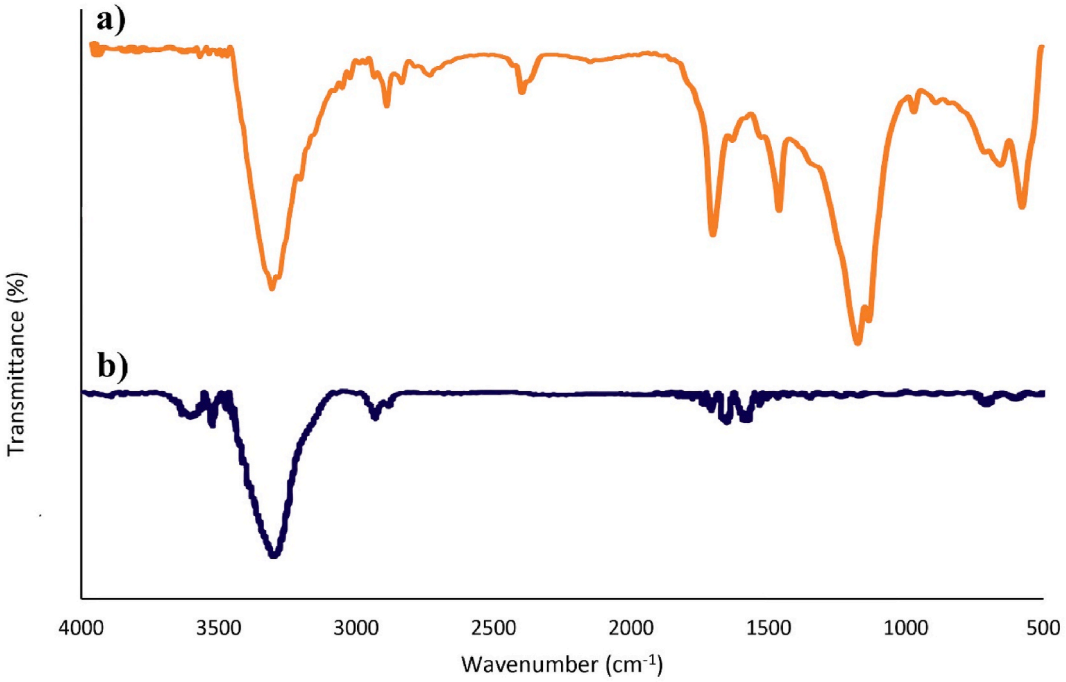

Fig. 15. FT-IR spectrum of (a) reused Ag@MC and (b) Ag@MC

4. Conclusion

In conclusion, the Ag@MC nanocomposite, synthesized using cherry tree gum, was effectively applied as a catalyst for reducing nitroaromatic compounds in the presence of hydrazine hydrate under microwave and solvent-free conditions. The Ag@MC nanocomposite exhibited high conversion efficiency for reducing various nitroaromatic compounds to aromatic amine products, thereby neutralizing their hazardous effects. The cherry tree gum, after being subjected to high temperatures in a furnace, proved to be an excellent carbon precursor for synthesizing microporous carbon due to its various monosaccharide compounds. Additionally, Ag@MC demonstrated impressive reusability, with no significant decrease in efficiency after being reused six times. These results highlight the potential of Ag@MC as a promising catalyst in various chemical applications.

CRediT authorship contribution statement

Hossein Ghafuri: Visualization, Supervision, Methodology, Investigation. **Fariba Gholipour:** Investigation, Formal analysis. **Peyman Hanifehnejad:** Writing – review & editing, Writing – original draft, Investigation, Data curation. **Fatemeh Bijari:** Writing – original draft, Data curation.

Data availability

Upon reasonable request, the corresponding author can provide access to the datasets utilized and/or analyzed during the course of this research.

Declaration of competing interest

The authors declare that they have no known competing financial interests or personal relationships that could have appeared to influence the work reported in this paper.

Appendix A. Supplementary data

Supplementary data to this article can be found online at https://doi.org/10.1016/j.heliyon.2025.e41961.

References

[1] E.K. Nti, et al., Water pollution control and revitalization using advanced technologies: uncovering artificial intelligence options towards environmental health protection, sustainability and water security, Heliyon 9 (7) (2023) e18170.
[2] I. Zahoor, et al., Water pollution from agricultural activities: a critical global review, Int. J. Chem. Biochem. Sci 23 (1) (2023) 164–176.
[3] F. Kordbacheh, et al., Water pollutants and approaches for their removal, Mater. Chem. Horizons 2 (2) (2023) 139–153.
[4] H. Solayman, et al., Performance evaluation of dye wastewater treatment technologies: a review, J. Environ. Chem. Eng. 11 (3) (2023) 109610.
[5] C. Yue, et al., Metal–organic framework-based materials: emerging high-efficiency catalysts for the heterogeneous photocatalytic degradation of pollutants in water, Environ. Sci.: Water Res. Technol. 9 (3) (2023) 669–695.
[6] P. Vivek, et al., Meticulous review on potential nano–sized catalysts for air and water purifiers, Iran. J. Catal. 11 (4) (2021) 331–345.
[7] U. Chakraborty, et al., Advanced metal oxides nanostructures to recognize and eradicate water pollutants, Prog. Mater. Sci. 139 (2023) 101169.
[8] L. Velarde, et al., Adsorption of heavy metals on natural zeolites: a review, Chemosphere 328 (2023) 138508.
[9] Y. Fu, et al., Recent progress of noble metals with tailored features in catalytic oxidation for organic pollutants degradation, J. Hazard Mater. 422 (2022) 126950.
[10] R. Suresh, et al., Enzyme Immobilized nanomaterials: an electrochemical bio-sensing and biocatalytic degradation properties toward organic pollutants, Top. Catal. 66 (9) (2023) 691–706.
[11] M. Dong, et al., Biochar for the removal of emerging pollutants from aquatic systems: a review, Int. J. Environ. Res. Publ. Health 20 (3) (2023) 1679.
[12] M. Zhang, et al., Porous carbon materials with different dimensions and their applications in supercapacitors, J. Phys. D Appl. Phys. (2024).
[13] H. Ghafuri, et al., Synthesis and characterization of nanocatalyst Cu2+/mesoporous carbon for amidation reactions of alcohols, Sci. Rep. 13 (1) (2023) 10133.
[14] A. Rashidizadeh, et al., Tandem oxidative amidation of alcohols catalyzed by copper modified well-ordered mesoporous graphitic carbon nitride, Solid State Sci. 109 (2020) 106427.
[15] S. De, et al., Biomass-derived porous carbon materials: synthesis and catalytic applications, ChemCatChem 7 (11) (2015) 1608–1629.
[16] H.B. Erdem, et al., Facile insitu preparation of silver nanoparticles supported on petroleum asphaltene-derived porous carbon for efficient reduction of nitrophenols, Heliyon 8 (9) (2022) e10659.
[17] K. Yang, et al., Enhanced functional properties of porous carbon materials as high-performance electrode materials for supercapacitors, Green Energy Resour (2023) 100030.
[18] Z. Pan, et al., Recent advances in porous carbon materials as electrodes for supercapacitors, Nanomaterials 13 (11) (2023) 1744.
[19] H. Shabani, et al., Sweet cherry tree (Prunus avium) exudate gum-based film modification in a photoreactor: effects of hydrogen peroxide oxidation, UV irradiation, and TiO2 nanoparticles, Int. J. Biol. Macromol. 266 (2024) 130932.
[20] H. Ghafuri, et al., Trimesic acid-modified magnetic gum as a highly efficient and recyclable biocatalyst for the one-pot green synthesis of condensation reactions, Int. J. Biol. Macromol. 227 (2023) 685–697.
[21] S. Ergin, et al., The usage of edible films extracted from cherry and apricot tree gums for coating of strawberry (Fragaria ananassa) and loquat (Eriobotrya japonica) fruits, Food Sci. Technol. 6 (5) (2018) 561–569.
[22] M. Olivares-Marín, et al., Preparation of activated carbon from cherry stones by chemical activation with ZnCl2, Appl. Surf. Sci. 252 (17) (2006) 5967–5971.
[23] J. Hwang, et al., Controlling the morphology of metal–organic frameworks and porous carbon materials: metal oxides as primary architecture-directing agents, Chem. Soc. Rev. 49 (11) (2020) 3348–3422.
[24] P. Veerakumar, et al., Research progress on porous carbon supported metal/metal oxide nanomaterials for supercapacitor electrode applications, Ind. Eng. Chem. Res. 59 (14) (2020) 6347–6374.
[25] A. Dhaka, et al., A review on biological synthesis of silver nanoparticles and their potential applications, Results Chem. (2023) 101108.
[26] F. Rodríguez-Félix, et al., Sustainable-green synthesis of silver nanoparticles using safflower (Carthamus tinctorius L.) waste extract and its antibacterial activity, Heliyon 7 (4) (2021) e06923.
[27] P. Kovacic, et al., Nitroaromatic compounds: environmental toxicity, carcinogenicity, mutagenicity, therapy and mechanism, J. Appl. Toxicol. 34 (8) (2014) 810–824.
[28] K.-S. Ju, R.E. Parales, Nitroaromatic compounds, from synthesis to biodegradation, Microbiol. Mol. Biol. Rev. 74 (2) (2010) 250–272.
[29] S. R Wilkinson, et al., Trypanocidal activity of nitroaromatic prodrugs: current treatments and future perspectives, Curr. Top. Med. Chem. 11 (16) (2011) 2072–2084.
[30] Y.M.A. Mohamed, et al., Palladium-Modified TiO2/MWCNTs for efficient carbon capture and photocatalytic reduction of nitro-aromatic derivatives, ChemistrySelect 8 (5) (2023) e202203098.
[31] L. Mavaddatiyan, et al., A new strategy for immobilization of copper on the Fe3O4@ EDTA nanocomposite and its efficient catalytic applications in reduction and one-pot reductive acetylation of nitroarenes and also N-acetylation of arylamines, Heliyon 10 (15) (2024) e35062.
[32] M. Zarei, et al., Fabrication of biochar@ Cu-Ni nanocatalyst for reduction of aryl aldehyde and nitroarene compounds, Biomass Convers. Biorefin. 14 (2) (2024) 2761–2776.
[33] T. Chen, et al., High-performance Pd nanoalloy on functionalized activated carbon for the hydrogenation of nitroaromatic compounds, J. Chem. Eng. 259 (2015) 161–169.
[34] S.U. Nandanwar, et al., Synthesis of colloidal CuO/γ-Al2O3 by microemulsion and its catalytic reduction of aromatic nitro compounds, Chin. J. Catal. 33 (9–10) (2012) 1532–1541.
[35] R. Millán, et al., A new molecular pathway allows the chemoselective reduction of nitroaromatics on non-noble metal catalysts, J. Catal. 364 (2018) 19–30.
[36] T. Wan, et al., Special direct route for efficient transfer hydrogenation of nitroarenes at room temperature by monatomic Zr tuned α-Fe2O3, J. Catal. 414 (2022) 245–256.
[37] M. Orlandi, et al., Recent developments in the reduction of aromatic and aliphatic nitro compounds to amines, Org. Process Res. Dev. 22 (4) (2016) 430–445.
[38] I. Kalavrouziotis, et al., The environmental impact of the platinum group elements (Pt, Pd, Rh) emitted by the automobile catalyst converters, Water Air Soil Pollut. 196 (2009) 393–402.
[39] J.L. Young, et al., Replacement of hazardous solvents and reagents in analytical chemistry. Challenges in Green Analytical Chemistry, 2011, pp. 44–62.
[40] H. Borna, et al., Using cherry tree sap to produce a natural coating film on the body surface to prevent sweating, J. Mar. Med. 2 (3) (2020) 171–180.
[41] S. Tan, et al., Facile fabrication of copper-supported ordered mesoporous carbon for antibacterial behavior, Mater. Lett. 64 (20) (2010) 2163–2166.
[42] K. Shameli, et al., Green biosynthesis of silver nanoparticles using Curcuma longa tuber powder, Int. J. Nanomed. (2012) 5603–5610.
[43] S.C. Rodrigues, et al., Use of magnetic activated carbon in a solid phase extraction procedure for analysis of 2, 4-dichlorophenol in water samples, Water, Air, Soil Pollut. 231 (2020) 1–13.
[44] L. Mulfinger, et al., Synthesis and study of silver nanoparticles, J. Chem. Educ. 84 (2) (2007) 322.
[45] P.R. Thombal, et al., Efficient metal-free catalytic reduction of Nitro to Amine over carbon sheets doped with Nitrogen, Catal. Lett. 152 (2) (2022) 538–546.
[46] S. Boycheva, et al., Surface studies of fly ash zeolites via adsorption/desorption isotherms, Bulg, Chem. Commun. 48 (2016) 101–107.
[47] U.T. Hwang, et al., Analysis of carbonization behavior of hydrochar produced by hydrothermal carbonization of lignin and development of a prediction model for carbonization degree using near-infrared spectroscopy, J. Korean Wood Sci. Technol. 49 (3) (2021) 213–225.
[48] Y. Zhang, et al., Alkaline potassium aluminum carbonate: a novel high-efficiency dry powder extinguishing agent with high heat-resistant, J. Anal. Appl. Pyrolysis 173 (2023) 106038.
[49] M. Gholinejad, et al., Hyperbranched polymer immobilized palladium nanoparticles as an efficient and reusable catalyst for cyanation of aryl halides and reduction of nitroarenes, J. Organomet. Chem. 970 (2022) 122359.
[50] I. Sagiv-Barfi, et al., Design, synthesis, and evaluation of quinazoline T cell proliferation inhibitors, Bioorg. Med. Chem. 18 (17) (2010) 6404–6413.

[51] A. Ghatak, et al., Chemoselective reduction of nitroaromatics using recyclable alumina-supported nickel nanoparticles in aqueous medium—exploration to one pot synthesis of benzimidazoles, Synth. Commun. 52 (3) (2022) 368–379.
[52] M. Rajabzadeh, et al., Generation of Cu nanoparticles on novel designed Fe 3 O 4@ SiO 2/EP. EN. EG as reusable nanocatalyst for the reduction of nitro compounds, RSC Adv. 6 (23) (2016) 19331–19340.
[53] H. Veisi, et al., Greener approach for synthesis of monodispersed palladium nanoparticles using aqueous extract of green tea and their catalytic activity for the Suzuki–Miyaura coupling reaction and the reduction of nitroarenes, Appl. Organomet. Chem. 31 (6) (2017) e3609.
[54] D.I. Ioannou, et al., Selective reduction of nitroarenes to arylamines by the cooperative action of methylhydrazine and a tris (N-heterocyclic thioamidate) cobalt (III) complex, J. Org. Chem. 86 (3) (2021) 2895–2906.
[55] J. Rahimi, et al., Enhanced reduction of nitrobenzene derivatives: effective strategy executed by Fe3O4/PVA-10% Ag as a versatile hybrid nanocatalyst, Catal. Commun. 134 (2020) 105850.
[56] M. Aidene, et al., Reactivity of 2, 1-benzisoxazole in palladium-catalyzed direct arylation with aryl bromides, ChemCatChem 8 (8) (2016) 1583–1590.
[57] P. Xu, et al., Magnetic separable chitosan microcapsules decorated with silver nanoparticles for catalytic reduction of 4-nitrophenol, J. Colloid Interface Sci. 507 (2017) 353–359.
[58] K. Hasan, et al., Magnetic chitosan-supported silver nanoparticles: a heterogeneous catalyst for the reduction of 4-nitrophenol, Catalyst 9 (10) (2019) 839.
[59] Y. Ling, et al., Quaternized chitosan/rectorite/AgNP nanocomposite catalyst for reduction of 4-nitrophenol, J. Alloys Compd. 647 (2015) 463–470.
[60] S. El-Hout, et al., A green chemical route for synthesis of graphene supported palladium nanoparticles: a highly active and recyclable catalyst for reduction of nitrobenzene, Appl. Catal. 503 (2015) 176–185.
[61] G. Grieco, et al., Microwave-assisted reduction of aromatic nitro compounds with novel oxo-rhenium complexes, Appl. Organomet. Chem. 36 (1) (2022) e6452.